Entropy Production of Nanosystems with Time Scale Separation

Shou-Wen Wang,[1,2] Kyogo Kawaguchi,[3] Shin-ichi Sasa,[4] and Lei-Han Tang[1,5]
[1]Beijing Computational Science Research Center, Beijing 100094, China
[2]Department of Engineering Physics, Tsinghua University, Beijing 100086, China
[3]Department of Systems Biology, Harvard Medical School, Boston, Massachusetts 02115, USA
[4]Department of Physics, Kyoto University, Kyoto 606-8502, Japan
[5]Department of Physics and Institute of Computational and Theoretical Studies, Hong Kong Baptist University, Hong Kong, China
(Received 16 January 2016; published 10 August 2016)

Energy flows in biomolecular motors and machines are vital to their function. Yet experimental observations are often limited to a small subset of variables that participate in energy transport and dissipation. Here we show, through a solvable Langevin model, that the seemingly hidden entropy production is measurable through the violation spectrum of the fluctuation-response relation of a slow observable. For general Markov systems with time scale separation, we prove that the violation spectrum exhibits a characteristic plateau in the intermediate frequency region. Despite its vanishing height, the plateau can account for energy dissipation over a broad time scale. Our findings suggest a general possibility to probe hidden entropy production in nanosystems without direct observation of fast variables.

DOI: 10.1103/PhysRevLett.117.070601

Introduction.—Recent advances in technology have made it possible to investigate energetic aspects of an open nanosystem experimentally. Studies have been carried out to quantify, e.g., the energy conversion efficiency of molecular motors [1,2], the information-energy conversion efficiency of an artificial Maxwell demon [3–6], the entropy production of a quantum tunneling device in a temperature gradient [7], and the effective temperature of single molecules in nonequilibrium steady states [8].

In the most interesting cases, such small systems are capable of complex dynamic behavior by virtue of multiple degrees of freedom over a broad range of time scales, and furthermore by operating out of equilibrium. The functional features of these systems are usually associated with slow processes, but recent theoretical studies have provided several examples of "hidden entropy production" arising from nonequilibrium coupling between fast and slow variables [9–19]. A better understanding of the conditions and key characteristics of this phenomenon is desirable not only from a theoretical viewpoint, but also for developing experimental protocols to uncover channels of energy dissipation without a full characterization of the possibly great many fast processes in a complex nanosystem.

In this Letter, we show that it is indeed possible to trace the hidden entropy production by quantifying the violation spectrum of the fluctuation-response relation (FRR) of a slow observable. In equilibrium systems, the FRR states that the spontaneous fluctuation of an observable decays in the same way as the deviation produced by an external perturbation. For a velocity observable $\dot{x}$ which is of particular interest here, the former can be measured via the autocorrelation function $C_{\dot{x}}(t) \equiv \langle [\dot{x}(t) - \langle \dot{x} \rangle_s][\dot{x}(0) - \langle \dot{x} \rangle_s] \rangle_s$ in the stationary ensemble $\langle \cdot \rangle_s$, while the latter is captured by the dynamic response $R_{\dot{x}}(t) \equiv \delta \langle \dot{x}(t) \rangle / \delta h$, with h being the perturbing field [20]. In frequency, $\tilde{C}_{\dot{x}}(\omega) = 2T\tilde{R}'_{\dot{x}}(\omega)$, where T is the temperature of the bath and the prime on $\tilde{R}_{\dot{x}}$ denotes its real part. However, the two properties are not simply related for nonequilibirum systems [21–24]. One significant result achieved in this direction is an equality derived by Harada and Sasa (HS) in Langevin systems. The equality connects the steady-state dissipation rate through the frictional motion of x, denoted as J_x, to the integral of the frequency-resolved FRR violation [25,26],

$$J_x = \gamma \left\{ \langle \dot{x} \rangle_s^2 + \int_{-\infty}^{\infty} \frac{d\omega}{2\pi} [\tilde{C}_{\dot{x}}(\omega) - 2T\tilde{R}'_{\dot{x}}(\omega)] \right\}, \quad (1)$$

where γ is the friction coefficient. This equality has been validated experimentally in a driven colloidal system [27], and applied to F_1-ATPase, a biomolecular motor, to infer the dissipation rate of the rotary motion [2,28].

The known applications of the HS equality are for systems that dissipate energy on a slow time scale. Here we show that the HS equality can also be used to probe hidden entropy production that takes place on time scales faster than the relaxation time of the observed variable. We first demonstrate, in a solvable Langevin model, the use of Eq. (1) to fully account for the dissipated energy in a nonequilibrium steady state. Interestingly, the FRR violation becomes vanishingly small for large time scale separation, while its integral with respect to frequency remains finite. We present a proof that this feature of the FRR violation spectrum, arising from the dissipative coupling between slow and fast variables, is generic for a time scale separated Markov system. Based on these findings, we suggest an experimental method to detect hidden entropy production from the fluctuation-response spectrum of a slow variable.

Potential switching model.—Consider the one-dimensional, over-damped motion of a bead subjected to a potential that switches stochastically between $U_0(x)$ and $U_1(x)$ at a rate r. Figure 1(a) illustrates an experimental realization using a laser trap that produces a harmonic potential $U_0(x) = kx^2/2$ whose center position switches back and forth between $x = 0$ and L [therefore $U_1(x) = k(x-L)^2/2$] [8,27]. This can also be viewed as a minimum Langevin model to study molecular machines which have fast binding or unbinding of currency molecules that triggers transition between different chemical states. With the potential state σ_t $(=0,1)$ at time t, and under a perturbing force h, the Langevin equation for the bead position x takes the form

$$\gamma\dot{x} = -\partial_x U_{\sigma_t}(x) + h(t) + \eta(t). \tag{2}$$

Here γ is the friction coefficient and $\eta(t)$ is the thermal noise satisfying $\langle\eta(t)\rangle = 0$ and $\langle\eta(t)\eta(t')\rangle = 2\gamma T\delta(t-t')$, with T the temperature of the bath. The Boltzmann constant k_B is set to 1.

The model defined above has two time scales, $\tau_s = \gamma/k$ for relaxation within a given potential and $\tau_f = 1/r$ for

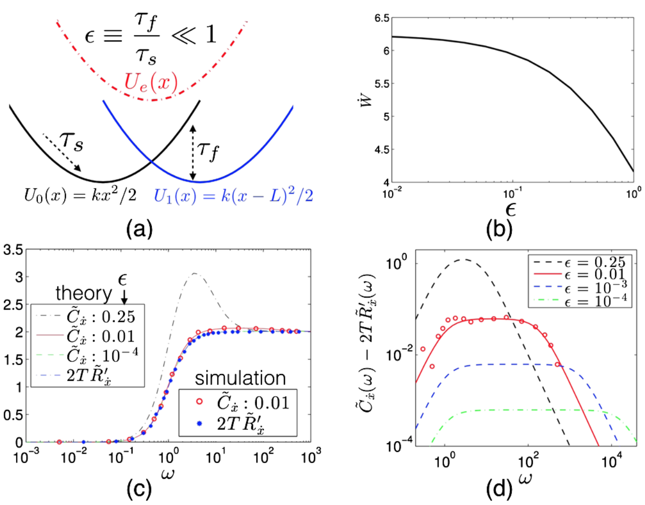

FIG. 1. (a) The potential switching model with a fast switching time constant $\tau_f = 1/r$ and a slow relaxation time constant $\tau_s = \gamma/k$. The effective potential $U_e(x)$ in the fast switching limit $\epsilon \ll 1$ is shown. (b) Rate of energy input against ϵ. (c) Frequency spectra of the velocity correlation and response functions at various values of ϵ. (d) Frequency spectra of the FRR violation whose integral yields the hidden entropy production that balances energy input in (b). Parameters: $k = \gamma = 1$ and $L = 5$. Open circles and stars in (c) and (d) give results from a simulated trajectory of length $T_{sp} = 10^4\tau_s$ and sampling rate $2\tau_f^{-1}$. The response function is reconstructed from data using a perturbation strength $h = 0.5$. (See Supplemental Material [29].)

potential switching. We introduce $\epsilon \equiv \tau_f/\tau_s$ to characterize the time scale separation between the two competing processes. In the fast switching limit $\epsilon \to 0$, it is straightforward to show that the steady-state distribution of the bead position takes the Boltzmann form $P^s(x) \sim \exp[-U_e(x)/T]$, where $U_e = [U_0(x) + U_1(x)]/2$ is the effective potential seen by the bead. Nevertheless, due to potential switching, energy is continuously injected into the system at an average rate

$$\dot{W} = \int_{-\infty}^{\infty} r[P_0^s(x) - P_1^s(x)][U_1(x) - U_0(x)]dx,$$

where $P_\sigma^s(x)$ is the stationary distribution in the full state space (x, σ). By analyzing the Fokker-Planck equation in the steady state satisfied by $P_\sigma^s(x)$, we obtain

$$\dot{W} \overset{\epsilon\to 0}{\to} \frac{1}{4\gamma}\langle\{\partial_x[U_1(x) - U_0(x)]\}^2\rangle_s \tag{3}$$

where $\langle\cdot\rangle_s$ denotes the average over the reduced distribution $P^s(x)$. In the case of a harmonic potential, Eq. (3) yields $\dot{W} = k^2L^2/(2\epsilon\gamma + 4\gamma)$. As shown in Fig. 1(b), the energy injection rate is always positive and approaches a constant in the limit $\epsilon \to 0$.

We now examine dissipation of the injected energy through viscous relaxation of the bead position x, which is our slow variable. To use Eq. (1) to compute the associated entropy production, we need to work out the velocity correlation spectrum $\tilde{C}_{\dot{x}}(\omega)$ and the response spectrum $\tilde{R}'_{\dot{x}}(\omega)$. It turns out that, in the harmonic case, Eq. (2) takes a linear form and can be solved analytically. Here, $\partial_x U_{\sigma_t}(x) = \partial_x U_e(x) - \xi(t)$ is decomposed into an effective force $\partial_x U_e(x) = k(x - L/2)$ and a "switching noise" $\xi(t) = kL(\sigma_t - 1/2)$, with $\langle\xi(t)\rangle = 0$ and $\langle\xi(t)\xi(t')\rangle = (kL/2)^2\exp(-2r|t-t'|)$. As shown in Fig. 1(c), $\tilde{R}'_{\dot{x}}(\omega) = \gamma\omega^2/(k^2 + \gamma^2\omega^2)$ is independent of ϵ. The correlation spectrum $\tilde{C}_{\dot{x}}(\omega)$, on the other hand, contains a term $2T\tilde{R}'_{\dot{x}}(\omega)$ from the thermal noise $\eta(t)$, and the remaining part from the switching noise $\xi(t)$. The latter is precisely the FRR violation spectrum shown in Fig. 1(d):

$$\tilde{C}_{\dot{x}}(\omega) - 2T\tilde{R}'_{\dot{x}}(\omega) = \epsilon\frac{k(L/2)^2}{1 + (\omega\tau_f/2)^2}\tilde{R}'_{\dot{x}}(\omega). \tag{4}$$

Carrying out the integral over ω in Eq. (1), we obtain $J_x = \dot{W}$. Therefore, the FRR violation spectrum of the slow variable $\dot{x}$ allows full recovery of entropy production in the present case.

A remarkable feature of the FRR violation spectrum displayed in Fig. 1(d), which is also evident from Eq. (4), is the plateau behavior in the intermediate frequency range $\tau_s^{-1} \ll \omega \ll \tau_f^{-1}$. This is the time or frequency window over which the fluctuating dynamics of x deviates most from equilibrium, and also where the hidden entropy production takes place in the model. As ϵ approaches zero, the height of the plateau diminishes, leaving the apparent impression that the FRR is restored. Nevertheless, the integral in Eq. (1) remains finite so as to be consistent with the energy input shown in Fig. 1(b). Our explicit solution of the potential switching model thus exposes subtleties surrounding the limit $\epsilon \to 0$.

The above example demonstrates that, with the help of the HS equality, at least part of the hidden entropy production can be recovered through precise measurement of the FRR violation spectrum of a slow variable. To gain an impression on the feasibility of this proposal, we have explicitly reconstructed the velocity correlation and response spectrum from a simulated stochastic trajectory $x(t)$ of the potential switching model at $\epsilon = 0.01$. The length of the trajectory is taken to be $T_{sp} = 10^4\tau_s$, with a sampling rate of $2\tau_f^{-1}$. This is sufficient to reveal the full range of the plateau as indicated by open circles in Fig. 1(d). As we show in the Supplemental Material [29], the relative fluctuation of $\tilde{C}(\omega)$ goes generally as $(T_{sp}/\tau_s)^{-1/2}$. Therefore, to reach a precision of order ϵ, the length of the time series should be of the order of τ_s/ϵ^2. Lowering temporal resolution in the measurement will lose information on the high frequency end of the spectrum. Nevertheless, even a sampling rate of $0.1\tau_f^{-1}$ can provide good evidence of nonequilibrium fluctuations in x generated by the hidden fast processes.

Below we show that the plateau behavior is a general feature of nonequilibrium Markov systems with time scale separation. Since a Langevin model can be considered as a special case of the Markov process, the aforementioned results can be extended to general potential switching models with a nonlinear force field and position-dependent switching rates, including the well-studied F_1-ATPase. This constitutes the main result.

General Markov processes.—Consider a general connected Markov system with N states. Transition from state m to state n ($1 \le n, m \le N$) takes place at rate w_m^n. The probability $P_n(t)$ to be at state n after time t follows the master equation

$$\frac{d}{dt}P_n(t) = \sum_m M_{nm}P_m(t), \tag{5}$$

where $M_{nm} = w_m^n - \delta_{nm}\sum_k w_n^k$ and δ_{nm} is the Kronecker delta. The right and left eigenmodes, denoted as x_j and y_j respectively, satisfy $\sum_m M_{nm}x_j(m) = -\lambda_j x_j(n)$ and $\sum_n y_j(n)M_{nm} = -\lambda_j y_j(m)$, where the minus sign is introduced so that $\mathrm{Re}(\lambda_j) \ge 0$. We rank λ_j in an ascending order by its real part, i.e., $\mathrm{Re}(\lambda_1) \le \mathrm{Re}(\lambda_2) \le \cdots$. The first eigenvalue $\lambda_1 = 0$, with $x_1(n) = P_n^s$ being the steady-state distribution and $y_1(n) = 1$. Generically, the normalized eigenmodes satisfy the orthogonality relation $\sum_n x_j(n)y_{j'}(n) = \delta_{jj'}$ and the completeness relation $\sum_j x_j(n)y_j(n') = \delta_{nn'}$.

We now introduce an external perturbation of strength h whose effect on the dynamics is specified by the modified transition rates $\tilde{w}_m^n = w_m^n \exp[(\mathcal{Q}_n - \mathcal{Q}_m)h/2T]$, where $\mathcal{Q}_n$ is a state variable conjugate to h [32,33]. Along a stochastic trajectory n_t, $Q(t) \equiv \mathcal{Q}_{n_t}$. In analogy with the velocity variable for the Langevin dynamics (2), we consider the time derivative $\dot{Q}(t)$ whose correlation and dynamic response are defined as $C_{\dot{Q}}(t-\tau) \equiv \langle[\dot{Q}(t) - \langle\dot{Q}\rangle_s][\dot{Q}(\tau) - \langle\dot{Q}\rangle_s]\rangle_s$ and $R_{\dot{Q}}(t-\tau) \equiv \delta\langle\dot{Q}(t)\rangle/\delta h_\tau$, respectively. By following the time evolution of the state probabilities $P_n(t)$ under the eigenmode expansion, we have obtained general expressions for $C_{\dot{Q}}$ and $R_{\dot{Q}}$ which take the following form in frequency:

$$\tilde{C}_{\dot{Q}}(\omega) = \sum_{j=2}^{N} 2\alpha_j\beta_j\lambda_j\left(1 - \frac{1}{1+(\omega/\lambda_j)^2}\right), \tag{6a}$$

$$\tilde{R}_{\dot{Q}}(\omega) = \sum_{j=2}^{N} \alpha_j\phi_j\left(1 - \frac{1-i(\omega/\lambda_j)}{1+(\omega/\lambda_j)^2}\right), \tag{6b}$$

where i is the imaginary unit.

The coefficients in Eqs. (6) are weighted averages of $\mathcal{Q}$, i.e., $\alpha_j \equiv \sum_n \mathcal{Q}_n x_j(n)$, $\beta_j \equiv \sum_n \mathcal{Q}_n y_j(n)P_n^s$, and $\phi_j \equiv \sum_n B_n y_j(n)$, with $B_n \equiv \sum_m[w_m^n P_m^s + w_n^m P_n^s](\mathcal{Q}_n - \mathcal{Q}_m)/2T$. They satisfy the general sum rule [34]

$$\sum_{j=2}^{N} \alpha_j(\lambda_j\beta_j - T\phi_j) = 0. \tag{7}$$

The detailed balance condition $w_m^n P_n^{eq} = w_m^n P_m^{eq}$ implies $\lambda_j\beta_j^{eq} = T\phi_j^{eq}$ for all j, and hence the FRR $\tilde{C}_{\dot{Q}}(\omega) = 2T\tilde{R}'_{\dot{Q}}(\omega)$. More generally, in the limit $\omega \to \infty$, $\tilde{C}_{\dot{Q}}(\infty) = 2T\tilde{R}'_{\dot{Q}}(\infty) = \mathrm{const}$ by virtue of the sum rule, confirming the behavior seen in Fig. 1(c) on the high frequency side.

We now apply the general results to a time scale separated system whose states can be partitioned into K subgroups or coarse-grained states, denoted as p or q. Each state n (m) is alternatively labeled by p_k (q_l), with k (l) for a microscopic state within p (q). Within a coarse-grained state, transitions are fast (time scale $\sim\tau_f$), whereas transitions across coarse-grained states are slow (time scale $\sim\tau_s$), as illustrated in Fig. 2(a). Formally, this condition amounts to the statement that the transition rate matrix is split into two parts:

$$M_{p_k q_l} = \epsilon^{-1}\delta_{pq}M_{kl}^q + M_{p_k q_l}^{(1)}, \tag{8}$$

where $\epsilon^{-1}M^q$ ($\epsilon \equiv \tau_f/\tau_s$) is the transition rate matrix within a coarse-grained state q while $M^{(1)}$ is for slow transitions

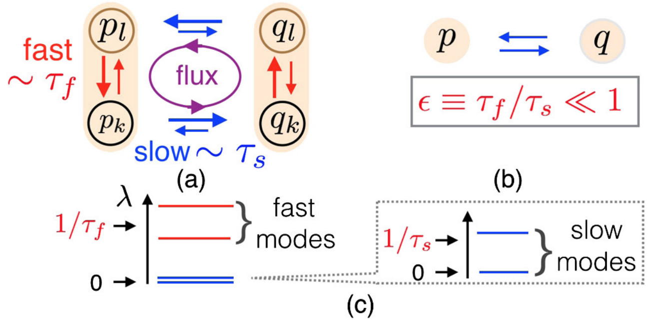

FIG. 2. (a) Illustration of a general nonequilibrium Markov process with a dissipative cycle formed by fast and slow processes. (b) Effective system at large time scale separation $\epsilon \ll 1$, where the circulating probability flux is hidden, along with the associated entropy production. (c) Eigenvalue spectrum of the master equation for a time scale separated system. Fast modes are well separated in their decay rates λ_j from the slow ones. The latter form a nearly degenerate band at the bottom that defines the slow dynamics of the effective system.

between coarse-grained states [35]. Below we shall analyze the eigenvalue and FRR spectra of the Markov process Eq. (8) using perturbation theory.

In the absence of intergroup transitions, the matrix M is block diagonalized. Within each block q, the rate matrix $\epsilon^{-1}M^q$ has a nondegenerate eigenvalue $\lambda_1^q = 0$ and the corresponding stationary distribution $P^s(l|q)$. All other eigenvalues of the matrix are positive and scale as ϵ^{-1}, which together define the fast modes of the system.

Figure 2(c) illustrates the eigenvalue spectrum of the block diagonalized matrix and its modification by $M^{(1)}$ when interblock transitions are introduced. Lifting of the K-fold degeneracy at $\lambda = 0$ can be analyzed using standard perturbation theory. To the leading order in ϵ, the projected transition rate matrix,

$$\hat{M}_{pq} = \sum_{k,l} M^{(1)}_{p_k q_l} P^s(l|q), \tag{9}$$

defines an emergent dynamics for the coarse-grained states. Its eigenmodes $\hat{x}_j$ and $\hat{y}_j$ with eigenvalue $\hat{\lambda}_j$ ($\sim$1) account for the leading order behavior of the slow modes ($j \le K$) in the full state space [34], which satisfy $x_j(p_k) = \hat{x}_j(p)P^s(k|p) + O(\epsilon)$, and $y_j(p_k) = \hat{y}_j(p) + O(\epsilon)$, and $\lambda_j = \hat{\lambda}_j + O(\epsilon)$. We now focus on a slow observable $Q_{p_k} = Q_p$ that only depends on the coarse-grained state. Then, $\hat{\alpha}_j$, $\hat{\beta}_j$, and $\hat{\phi}_j$ are also defined for the slow modes ($j \le K$), which turns out to be $\alpha_j = \hat{\alpha}_j + O(\epsilon)$, $\beta_j = \hat{\beta}_j + O(\epsilon)$, and $\phi_j = \hat{\phi}_j + O(\epsilon)$. In terms of the parameters from the coarse-grained dynamics, we may write

$$\tilde{C}_{\dot{Q}} - 2T\tilde{R}'_{\dot{Q}} = 2\sum_{j=2}^{K} \hat{\alpha}_j \frac{T\hat{\phi}_j - \hat{\beta}_j\hat{\lambda}_j}{1 + (\omega/\hat{\lambda}_j)^2} + \epsilon V_s(\omega). \tag{10}$$

An explicit form for $V_s(\omega)$ is given in the Supplemental Material [29]. In the intermediate region ($\tau_s^{-1} \ll \omega \ll \tau_f^{-1} \sim \epsilon^{-1}$), $V_s(\omega) \simeq 2\epsilon^{-1}\Sigma_{j=2}^{K}\alpha_j(\beta_j\lambda_j - T\phi_j) \xrightarrow{\epsilon\to 0}$ const due to the sum rule $\sum_{j=2}^{K}\hat{\alpha}_j(\hat{\beta}_j\hat{\lambda}_j - T\hat{\phi}_j) = 0$ under $\hat{M}$. Besides, $V_s(\omega)$ vanishes for both $\omega \gg \tau_f^{-1}$ and $\omega \ll \tau_s^{-1}$.

Equation (10) is the generalized description of the plateau behavior we found in the potential switching model [see Eq. (4)]. The low frequency FRR violation spectrum ($\omega \sim \tau_s^{-1}$) comes from the coarse-grained dynamics, which vanishes if the detailed balance condition is fulfilled under $\hat{M}$. In the intermediate frequency region, the nonequilibrium coupling between the fast and slow variables produces a plateau ϵV_s whose height diminishes in the time scale separation limit $\epsilon \to 0$.

Since the HS equality holds generally for system variables that follow the Langevin dynamics, Eq. (10) can be immediately used to obtain heat dissipation associated with the frictional motion of these variables. On the other hand, if the slow variable p takes on a discrete set of values, then the situation is more complicated. Lippiello *et al.* [36] considered a special class of discrete models whose dynamics follows closely that of a Langevin system. There it was shown for a one-dimensional system that, when the allowed transition rates take the symmetric form $w_m^n = \tau^{-1}e^{[S(n)-S(m)]/2}$ with $|S(n) - S(m)| \ll 1$, the HS equality holds approximately, and hence a link between the FRR violation spectrum and the heat dissipation can again be established. In the Supplemental Material [29], we present an example with a ladder network structure. More general discussion of the relation between the plateau behavior and the hidden entropy production is left to future work.

Concluding Remarks.—We have demonstrated in a fairly general setting that, for driven systems with large time scale separation, the fluctuation-response relation applied to a slow variable is close to being satisfied below its relaxation time. However, close examination should reveal a characteristic plateau behavior in the FRR violation spectrum in the intermediate frequency region. The Harada-Sasa equality can then be invoked to compute the frictional dissipation arising from nonequilibrium fluctuations using data from precise measurements of the fluctuation-response spectrum.

We believe that our findings can be applied to expose hidden entropy production in molecular motors. Examples include the F_1-ATPase mutants [37,38], which are known to be less efficient in converting chemical to mechanical energy as compared to the wild type. The fast variable in this case corresponds to the chemical states associated with ATP binding and hydrolysis, while the relatively slow variable is the rotational angle. Their chemomechanical coupling is usually modeled by a potential switching model where position-dependent ATP binding and hydrolysis shifts the potential forward, thus generating a directed rotation [28]. Our work suggests that energy loss in inefficient motors may be caused by fast switching of the chemical states that produces nonequilibrium fluctuations in the rotary motion. If so, at least part of the hidden entropy production can be measured by observing the rotary motion with a high speed camera, without monitoring the chemical states. Suppose that the rotary motion has a relaxation time around 0.1 s, and the time scale of ATP binding or hydrolysis around 5×10^{-3} s, then a sampling duration $T_{sp} = 400$ s and a temporal resolution 2.5×10^{-3} s, which is attainable in state-of-the-art single molecule experiments [39], would be enough to see the FRR violation spectrum. The rate of ATP binding and ADP release can be modified by varying the concentration of these molecules, yielding further information on the nature of nonequilibrium fluctuations and associated energy dissipation in the system.

The authors thank Yohei Nakayama and Takayuki Ariga for helpful suggestions on the manuscript. The work was supported in part by the NSFC (No. U1430237 and No. U1530401) and by the RGC of the Hong Kong Special Administrative Region (No. 12301514). It was also supported by KAKENHI (No. 25103002 and No. 26610115), by the JSPS Core-to-Core program "Nonequilibrium dynamics of soft-matter and information", and by the Grant-in-Aid for JSPS Fellows (No. 28-908).

[1] H. Noji, R. Yasuda, M. Yoshida, and K. Kinosita, Nature (London) **386**, 299 (1997).
[2] S. Toyabe, T. Okamoto, T. Watanabe-Nakayama, H. Taketani, S. Kudo, and E. Muneyuki, Phys. Rev. Lett. **104**, 198103 (2010).
[3] T. Sagawa and M. Ueda, Phys. Rev. Lett. **104**, 090602 (2010).
[4] S. Toyabe, T. Sagawa, M. Ueda, E. Muneyuki, and M. Sano, Nat. Phys. **6**, 988 (2010).
[5] A. Bérut A. Arakelyan, A. Petrosyan, S. Ciliberto, R. Dillenschneider, and E. Lutz, Nature (London) **483**, 187 (2012).
[6] J. V. Koski, A. Kutvonen, I. M. Khaymovich, T. Ala-Nissila, and J. P. Pekola, Phys. Rev. Lett. **115**, 260602 (2015).
[7] J. V. Koski, T. Sagawa, O. Saira, Y. Yoon, A. Kutvonen, P. Solinas, M. Möttönen, T. Ala-Nissila, and J. Pekola, Nat. Phys. **9**, 644 (2013).
[8] E. Dieterich, J. Camunas-Soler, M. Ribezzi-Crivellari, U. Seifert, and F. Ritort, Nat. Phys. **11**, 971 (2015).
[9] T. Hondou and K. Sekimoto, Phys. Rev. E **62**, 6021 (2000).
[10] M. Esposito, Phys. Rev. E **85**, 041125 (2012).
[11] A. Celani, S. Bo, R. Eichhorn, and E. Aurell, Phys. Rev. Lett. **109**, 260603 (2012).
[12] K. Kawaguchi and Y. Nakayama, Phys. Rev. E **88**, 022147 (2013).
[13] Y. Nakayama and K. Kawaguchi, Phys. Rev. E **91**, 012115 (2015).
[14] H.-M. Chun and J. D. Noh, Phys. Rev. E **91**, 052128 (2015).
[15] M. Esposito and J. M. R. Parrondo, Phys. Rev. E **91**, 052114 (2015).
[16] S.-W. Wang, Y. Lan, and L.-H. Tang, J. Stat. Mech. (2015) P07025.
[17] P. Sartori and Y. Tu, Phys. Rev. Lett. **115**, 118102 (2015).
[18] S. Bo and A. Celani, J. Stat. Phys. **154**, 1325 (2014).
[19] A. Puglisi, S. Pigolotti, L. Rondoni, and A. Vulpiani, J. Stat. Mech. (2010) P05015.
[20] R. Kubo, Rep. Prog. Phys. **29**, 255 (1966).
[21] L. F. Cugliandolo, D. S. Dean, and J. Kurchan, Phys. Rev. Lett. **79**, 2168 (1997).
[22] T. Speck and U. Seifert, Europhys. Lett. **74**, 391 (2006).
[23] M. Baiesi, C. Maes, and B. Wynants, Phys. Rev. Lett. **103**, 010602 (2009).
[24] U. Seifert and T. Speck, Europhys. Lett. **89**, 10007 (2010).
[25] T. Harada and S.-i. Sasa, Phys. Rev. Lett. **95**, 130602 (2005).
[26] T. Harada and S.-i. Sasa, Phys. Rev. E **73**, 026131 (2006).
[27] S. Toyabe, H.-R. Jiang, T. Nakamura, Y. Murayama, and M. Sano, Phys. Rev. E **75**, 011122 (2007).
[28] K. Kawaguchi, S.-i. Sasa, and T. Sagawa, Biophys. J. **106**, 2450 (2014).
[29] See Supplemental Material at http://link.aps.org/supplemental/10.1103/PhysRevLett.117.070601, which includes Ref. [30,31], for details of time-series data analysis protocols, the Harada-Sasa equality as an estimate of energy dissipation in discrete Markov systems, and derivation of Eq. (10).
[30] K. Berg-Sørensen and H. Flyvbjerg, Rev. Sci. Instrum. **75**, 594 (2004).
[31] Y. Tu, Annu. Rev. Biophys. **42**, 337 (2013).
[32] G. Diezemann, Phys. Rev. E **72**, 011104 (2005).
[33] C. Maes and B. Wynants, Markov Process. Relat. Fields **16**, 45 (2010).
[34] S.-W. Wang, K. Kawaguchi, S.-i. Sasa, and L.-H. Tang (unpublished).
[35] Aspects of such a time scale separated system was studied previously by S. Rahav and C. Jarzynski, J. Stat. Mech. (2007) P09012.
[36] E. Lippiello, M. Baiesi, and A. Sarracino, Phys. Rev. Lett. **112**, 140602 (2014).
[37] S. Toyabe, T. Watanabe-Nakayama, T. Okamoto, S. Kudo, and E. Muneyuki, Proc. Natl. Acad. Sci. U.S.A. **108**, 17951 (2011).
[38] S. Toyabe and E. Muneyuki, New J. Phys. **17**, 015008 (2015).
[39] S. Toyabe, H. Ueno, and E. Muneyuki, Europhys. Lett. **97**, 40004 (2012).